Fermilab-Pub-08/508-E

Search for the lightest scalar top quark in events with two leptons in $p\bar{p}$ collisions at $\sqrt{s} = 1.96$ TeV

V.M. Abazov[36], B. Abbott[75], M. Abolins[65], B.S. Acharya[29], M. Adams[51], T. Adams[49], E. Aguilo[6], M. Ahsan[59], G.D. Alexeev[36], G. Alkhazov[40], A. Alton[64,a], G. Alverson[63], G.A. Alves[2], M. Anastasoaie[35], L.S. Ancu[35], T. Andeen[53], B. Andrieu[17], M.S. Anzelc[53], M. Aoki[50], Y. Arnoud[14], M. Arov[60], M. Arthaud[18], A. Askew[49,b], B. Åsman[41], A.C.S. Assis Jesus[3], O. Atramentov[49], C. Avila[8], F. Badaud[13], L. Bagby[50], B. Baldin[50], D.V. Bandurin[59], P. Banerjee[29], S. Banerjee[29], E. Barberis[63], A.-F. Barfuss[15], P. Bargassa[80], P. Baringer[58], J. Barreto[2], J.F. Bartlett[50], U. Bassler[18], D. Bauer[43], S. Beale[6], A. Bean[58], M. Begalli[3], M. Begel[73], C. Belanger-Champagne[41], L. Bellantoni[50], A. Bellavance[50], J.A. Benitez[65], S.B. Beri[27], G. Bernardi[17], R. Bernhard[23], I. Bertram[42], M. Besançon[18], R. Beuselinck[43], V.A. Bezzubov[39], P.C. Bhat[50], V. Bhatnagar[27], G. Blazey[52], F. Blekman[43], S. Blessing[49], K. Bloom[67], A. Boehnlein[50], D. Boline[62], T.A. Bolton[59], E.E. Boos[38], G. Borissov[42], T. Bose[77], A. Brandt[78], R. Brock[65], G. Brooijmans[70], A. Bross[50], D. Brown[81], X.B. Bu[7], N.J. Buchanan[49], D. Buchholz[53], M. Buehler[81], V. Buescher[22], V. Bunichev[38], S. Burdin[42,c], T.H. Burnett[82], C.P. Buszello[43], P. Calfayan[25], S. Calvet[16], J. Cammin[71], M.A. Carrasco-Lizarraga[33], E. Carrera[49], W. Carvalho[3], B.C.K. Casey[50], H. Castilla-Valdez[33], S. Chakrabarti[72], D. Chakraborty[52], K.M. Chan[55], A. Chandra[48], E. Cheu[45], D.K. Cho[62], S. Choi[32], B. Choudhary[28], L. Christofek[77], T. Christoudias[43], S. Cihangir[50], D. Claes[67], J. Clutter[58], M. Cooke[50], W.E. Cooper[50], M. Corcoran[80], F. Couderc[18], M.-C. Cousinou[15], S. Crépé-Renaudin[14], V. Cuplov[59], D. Cutts[77], M. Ćwiok[30], H. da Motta[2], A. Das[45], G. Davies[43], K. De[78], S.J. de Jong[35], E. De La Cruz-Burelo[33], C. De Oliveira Martins[3], K. DeVaughan[67], F. Déliot[18], M. Demarteau[50], R. Demina[71], D. Denisov[50], S.P. Denisov[39], S. Desai[50], H.T. Diehl[50], M. Diesburg[50], A. Dominguez[67], T. Dorland[82], A. Dubey[28], L.V. Dudko[38], L. Duflot[16], S.R. Dugad[29], D. Duggan[49], A. Duperrin[15], S. Dutt[27], J. Dyer[65], A. Dyshkant[52], M. Eads[67], D. Edmunds[65], J. Ellison[48], V.D. Elvira[50], Y. Enari[77], S. Eno[61], P. Ermolov[38,‡], H. Evans[54], A. Evdokimov[73], V.N. Evdokimov[39], A.V. Ferapontov[59], T. Ferbel[61,71], F. Fiedler[24], F. Filthaut[35], W. Fisher[50], H.E. Fisk[50], M. Fortner[52], H. Fox[42], S. Fu[50], S. Fuess[50], T. Gadfort[70], C.F. Galea[35], C. Garcia[71], A. Garcia-Bellido[71], V. Gavrilov[37], P. Gay[13], W. Geist[19], W. Geng[15,65], C.E. Gerber[51], Y. Gershtein[49,b], D. Gillberg[6], G. Ginther[71], B. Gómez[8], A. Goussiou[82], P.D. Grannis[72], H. Greenlee[50], Z.D. Greenwood[60], E.M. Gregores[4], G. Grenier[20], Ph. Gris[13], J.-F. Grivaz[16], A. Grohsjean[25], S. Grünendahl[50], M.W. Grünewald[30], F. Guo[72], J. Guo[72], G. Gutierrez[50], P. Gutierrez[75], A. Haas[70], N.J. Hadley[61], P. Haefner[25], S. Hagopian[49], J. Haley[68], I. Hall[65], R.E. Hall[47], L. Han[7], K. Harder[44], A. Harel[71], J.M. Hauptman[57], J. Hays[43], T. Hebbeker[21], D. Hedin[52], J.G. Hegeman[34], A.P. Heinson[48], U. Heintz[62], C. Hensel[22,d], K. Herner[72], G. Hesketh[63], M.D. Hildreth[55], R. Hirosky[81], T. Hoang[49], J.D. Hobbs[72], B. Hoeneisen[12], M. Hohlfeld[22], S. Hossain[75], P. Houben[34], Y. Hu[72], Z. Hubacek[10], V. Hynek[9], I. Iashvili[69], R. Illingworth[50], A.S. Ito[50], S. Jabeen[62], M. Jaffré[16], S. Jain[75], K. Jakobs[23], C. Jarvis[61], R. Jesik[43], K. Johns[45], C. Johnson[70], M. Johnson[50], D. Johnston[67], A. Jonckheere[50], P. Jonsson[43], A. Juste[50], E. Kajfasz[15], D. Karmanov[38], P.A. Kasper[50], I. Katsanos[70], V. Kaushik[78], R. Kehoe[79], S. Kermiche[15], N. Khalatyan[50], A. Khanov[76], A. Kharchilava[69], Y.N. Kharzheev[36], D. Khatidze[70], T.J. Kim[31], M.H. Kirby[53], M. Kirsch[21], B. Klima[50], J.M. Kohli[27], J.-P. Konrath[23], A.V. Kozelov[39], J. Kraus[65], T. Kuhl[24], A. Kumar[69], A. Kupco[11], T. Kurča[20], V.A. Kuzmin[38], J. Kvita[9], F. Lacroix[13], D. Lam[55], S. Lammers[70], G. Landsberg[77], P. Lebrun[20], W.M. Lee[50], A. Leflat[38], J. Lellouch[17], J. Li[78,‡], L. Li[48], Q.Z. Li[50], S.M. Lietti[5], J.K. Lim[31], J.G.R. Lima[52], D. Lincoln[50], J. Linnemann[65], V.V. Lipaev[39], R. Lipton[50], Y. Liu[7], Z. Liu[6], A. Lobodenko[40], M. Lokajicek[11], P. Love[42], H.J. Lubatti[82], R. Luna-Garcia[33,e], A.L. Lyon[50], A.K.A. Maciel[2], D. Mackin[80], R.J. Madaras[46], P. Mättig[26], A. Magerkurth[64], P.K. Mal[82], H.B. Malbouisson[3], S. Malik[67], V.L. Malyshev[36], Y. Maravin[59], B. Martin[14], R. McCarthy[72], M.M. Meijer[35], A. Melnitchouk[66], L. Mendoza[8], P.G. Mercadante[5], M. Merkin[38], K.W. Merritt[50], A. Meyer[21], J. Meyer[22,d], J. Mitrevski[70], R.K. Mommsen[44], N.K. Mondal[29], R.W. Moore[6], T. Moulik[58], G.S. Muanza[15], M. Mulhearn[70], O. Mundal[22], L. Mundim[3], E. Nagy[15], M. Naimuddin[50], M. Narain[77], H.A. Neal[64], J.P. Negret[8], P. Neustroev[40], H. Nilsen[23], H. Nogima[3], S.F. Novaes[5], T. Nunnemann[25], D.C. O'Neil[6], G. Obrant[40], C. Ochando[16], D. Onoprienko[59], N. Oshima[50], N. Osman[43], J. Osta[55], R. Otec[10], G.J. Otero y Garzón[50], M. Owen[44], P. Padley[80], M. Pangilinan[77], N. Parashar[56], S.-J. Park[22,d], S.K. Park[31], J. Parsons[70], R. Partridge[77], N. Parua[54], A. Patwa[73], G. Pawloski[80], B. Penning[23], M. Perfilov[38], K. Peters[44], Y. Peters[26], P. Pétroff[16], M. Petteni[43], R. Piegaia[1], J. Piper[65], M.-A. Pleier[22], P.L.M. Podesta-Lerma[33,f], V.M. Podstavkov[50],

Y. Pogorelov[55], M.-E. Pol[2], P. Polozov[37], B.G. Pope[65], A.V. Popov[39], C. Potter[6], W.L. Prado da Silva[3], H.B. Prosper[49], S. Protopopescu[73], J. Qian[64], A. Quadt[22,d], B. Quinn[66], A. Rakitine[42], M.S. Rangel[2], K. Ranjan[28], P.N. Ratoff[42], P. Renkel[79], P. Rich[44], M. Rijssenbeek[72], I. Ripp-Baudot[19], F. Rizatdinova[76], S. Robinson[43], R.F. Rodrigues[3], M. Rominsky[75], C. Royon[18], P. Rubinov[50], R. Ruchti[55], G. Safronov[37], G. Sajot[14], A. Sánchez-Hernández[33], M.P. Sanders[17], B. Sanghi[50], G. Savage[50], L. Sawyer[60], T. Scanlon[43], D. Schaile[25], R.D. Schamberger[72], Y. Scheglov[40], H. Schellman[53], T. Schliephake[26], S. Schlobohm[82], C. Schwanenberger[44], A. Schwartzman[68], R. Schwienhorst[65], J. Sekaric[49], H. Severini[75], E. Shabalina[51], M. Shamim[59], V. Shary[18], A.A. Shchukin[39], R.K. Shivpuri[28], V. Siccardi[19], V. Simak[10], V. Sirotenko[50], P. Skubic[75], P. Slattery[71], D. Smirnov[55], G.R. Snow[67], J. Snow[74], S. Snyder[73], S. Söldner-Rembold[44], L. Sonnenschein[17], A. Sopczak[42], M. Sosebee[78], K. Soustruznik[9], B. Spurlock[78], J. Stark[14], V. Stolin[37], D.A. Stoyanova[39], J. Strandberg[64], S. Strandberg[41], M.A. Strang[69], E. Strauss[72], M. Strauss[75], R. Ströhmer[25], D. Strom[53], L. Stutte[50], S. Sumowidagdo[49], P. Svoisky[35], A. Sznajder[3], A. Tanasijczuk[1], W. Taylor[6], B. Tiller[25], F. Tissandier[13], M. Titov[18], V.V. Tokmenin[36], I. Torchiani[23], D. Tsybychev[72], B. Tuchming[18], C. Tully[68], P.M. Tuts[70], R. Unalan[65], L. Uvarov[40], S. Uvarov[40], S. Uzunyan[52], B. Vachon[6], P.J. van den Berg[34], R. Van Kooten[54], W.M. van Leeuwen[34], N. Varelas[51], E.W. Varnes[45], I.A. Vasilyev[39], P. Verdier[20], L.S. Vertogradov[36], M. Verzocchi[50], D. Vilanova[18], F. Villeneuve-Seguier[43], P. Vint[43], P. Vokac[10], M. Voutilainen[67,g], R. Wagner[68], H.D. Wahl[49], M.H.L.S. Wang[50], J. Warchol[55], G. Watts[82], M. Wayne[55], G. Weber[24], M. Weber[50,h], L. Welty-Rieger[54], A. Wenger[23,i], N. Wermes[22], M. Wetstein[61], A. White[78], D. Wicke[26], M.R.J. Williams[42], G.W. Wilson[58], S.J. Wimpenny[48], M. Wobisch[60], D.R. Wood[63], T.R. Wyatt[44], Y. Xie[77], C. Xu[64], S. Yacoob[53], R. Yamada[50], W.-C. Yang[44], T. Yasuda[50], Y.A. Yatsunenko[36], H. Yin[7], K. Yip[73], H.D. Yoo[77], S.W. Youn[53], J. Yu[78], C. Zeitnitz[26], S. Zelitch[81], T. Zhao[82], B. Zhou[64], J. Zhu[72], M. Zielinski[71], D. Zieminska[54], A. Zieminski[54,‡], L. Zivkovic[70], V. Zutshi[52], and E.G. Zverev[38]

(The DØ Collaboration)

[1] *Universidad de Buenos Aires, Buenos Aires, Argentina*
[2] *LAFEX, Centro Brasileiro de Pesquisas Físicas, Rio de Janeiro, Brazil*
[3] *Universidade do Estado do Rio de Janeiro, Rio de Janeiro, Brazil*
[4] *Universidade Federal do ABC, Santo André, Brazil*
[5] *Instituto de Física Teórica, Universidade Estadual Paulista, São Paulo, Brazil*
[6] *University of Alberta, Edmonton, Alberta, Canada, Simon Fraser University, Burnaby, British Columbia, Canada, York University, Toronto, Ontario, Canada, and McGill University, Montreal, Quebec, Canada*
[7] *University of Science and Technology of China, Hefei, People's Republic of China*
[8] *Universidad de los Andes, Bogotá, Colombia*
[9] *Center for Particle Physics, Charles University, Prague, Czech Republic*
[10] *Czech Technical University, Prague, Czech Republic*
[11] *Center for Particle Physics, Institute of Physics, Academy of Sciences of the Czech Republic, Prague, Czech Republic*
[12] *Universidad San Francisco de Quito, Quito, Ecuador*
[13] *LPC, Université Blaise Pascal, CNRS/IN2P3, Clermont, France*
[14] *LPSC, Université Joseph Fourier Grenoble 1, CNRS/IN2P3, Institut National Polytechnique de Grenoble, Grenoble, France*
[15] *CPPM, Aix-Marseille Université, CNRS/IN2P3, Marseille, France*
[16] *LAL, Université Paris-Sud, IN2P3/CNRS, Orsay, France*
[17] *LPNHE, IN2P3/CNRS, Universités Paris VI and VII, Paris, France*
[18] *CEA, Irfu, SPP, Saclay, France*
[19] *IPHC, Université Louis Pasteur, CNRS/IN2P3, Strasbourg, France*
[20] *IPNL, Université Lyon 1, CNRS/IN2P3, Villeurbanne, France and Université de Lyon, Lyon, France*
[21] *III. Physikalisches Institut A, RWTH Aachen University, Aachen, Germany*
[22] *Physikalisches Institut, Universität Bonn, Bonn, Germany*
[23] *Physikalisches Institut, Universität Freiburg, Freiburg, Germany*
[24] *Institut für Physik, Universität Mainz, Mainz, Germany*
[25] *Ludwig-Maximilians-Universität München, München, Germany*
[26] *Fachbereich Physik, University of Wuppertal, Wuppertal, Germany*
[27] *Panjab University, Chandigarh, India*
[28] *Delhi University, Delhi, India*
[29] *Tata Institute of Fundamental Research, Mumbai, India*
[30] *University College Dublin, Dublin, Ireland*

[31]Korea Detector Laboratory, Korea University, Seoul, Korea
[32]SungKyunKwan University, Suwon, Korea
[33]CINVESTAV, Mexico City, Mexico
[34]FOM-Institute NIKHEF and University of Amsterdam/NIKHEF, Amsterdam, The Netherlands
[35]Radboud University Nijmegen/NIKHEF, Nijmegen, The Netherlands
[36]Joint Institute for Nuclear Research, Dubna, Russia
[37]Institute for Theoretical and Experimental Physics, Moscow, Russia
[38]Moscow State University, Moscow, Russia
[39]Institute for High Energy Physics, Protvino, Russia
[40]Petersburg Nuclear Physics Institute, St. Petersburg, Russia
[41]Lund University, Lund, Sweden, Royal Institute of Technology and Stockholm University, Stockholm, Sweden, and Uppsala University, Uppsala, Sweden
[42]Lancaster University, Lancaster, United Kingdom
[43]Imperial College, London, United Kingdom
[44]University of Manchester, Manchester, United Kingdom
[45]University of Arizona, Tucson, Arizona 85721, USA
[46]Lawrence Berkeley National Laboratory and University of California, Berkeley, California 94720, USA
[47]California State University, Fresno, California 93740, USA
[48]University of California, Riverside, California 92521, USA
[49]Florida State University, Tallahassee, Florida 32306, USA
[50]Fermi National Accelerator Laboratory, Batavia, Illinois 60510, USA
[51]University of Illinois at Chicago, Chicago, Illinois 60607, USA
[52]Northern Illinois University, DeKalb, Illinois 60115, USA
[53]Northwestern University, Evanston, Illinois 60208, USA
[54]Indiana University, Bloomington, Indiana 47405, USA
[55]University of Notre Dame, Notre Dame, Indiana 46556, USA
[56]Purdue University Calumet, Hammond, Indiana 46323, USA
[57]Iowa State University, Ames, Iowa 50011, USA
[58]University of Kansas, Lawrence, Kansas 66045, USA
[59]Kansas State University, Manhattan, Kansas 66506, USA
[60]Louisiana Tech University, Ruston, Louisiana 71272, USA
[61]University of Maryland, College Park, Maryland 20742, USA
[62]Boston University, Boston, Massachusetts 02215, USA
[63]Northeastern University, Boston, Massachusetts 02115, USA
[64]University of Michigan, Ann Arbor, Michigan 48109, USA
[65]Michigan State University, East Lansing, Michigan 48824, USA
[66]University of Mississippi, University, Mississippi 38677, USA
[67]University of Nebraska, Lincoln, Nebraska 68588, USA
[68]Princeton University, Princeton, New Jersey 08544, USA
[69]State University of New York, Buffalo, New York 14260, USA
[70]Columbia University, New York, New York 10027, USA
[71]University of Rochester, Rochester, New York 14627, USA
[72]State University of New York, Stony Brook, New York 11794, USA
[73]Brookhaven National Laboratory, Upton, New York 11973, USA
[74]Langston University, Langston, Oklahoma 73050, USA
[75]University of Oklahoma, Norman, Oklahoma 73019, USA
[76]Oklahoma State University, Stillwater, Oklahoma 74078, USA
[77]Brown University, Providence, Rhode Island 02912, USA
[78]University of Texas, Arlington, Texas 76019, USA
[79]Southern Methodist University, Dallas, Texas 75275, USA
[80]Rice University, Houston, Texas 77005, USA
[81]University of Virginia, Charlottesville, Virginia 22901, USA and
[82]University of Washington, Seattle, Washington 98195, USA

(Dated: November 4, 2008)

We report results of a search for the pair production of the lightest supersymmetric partner of the top quark, $\tilde{t}_1$, using 1 fb^{-1} of data collected by the D0 detector at a $p\bar{p}$ center-of-mass energy of 1.96 TeV at the Fermilab Tevatron Collider. Both scalar top quarks are assumed to decay into a b quark, a charged lepton and a scalar neutrino. The search is performed in the electron plus muon and dielectron final states. The signal topology consists of two isolated leptons, missing transverse energy, and jets. We find no evidence for this process and exclude regions of parameter space in the framework of the minimal supersymmetric standard model.

PACS numbers: 14.80.Ly, 12.60.Jv, 13.85.Rm

Supersymmetric theories [1] predict for every standard model (SM) particle the existence of a superpartner that differs by half a unit of spin. The top quark would have two scalar partners, $\tilde{t}_L$ and $\tilde{t}_R$, corresponding to its left and right handed states. Mixing between $\tilde{t}_L$ and $\tilde{t}_R$, being proportional to the top quark mass m_t, may lead to a possible large mass splitting between the physical states $\tilde{t}_1$ and $\tilde{t}_2$. Hence, the lightest supersymmetric partner of the top quark, $\tilde{t}_1$, might be light enough to be produced at the Fermilab Tevatron collider.

In this Letter we present a search for scalar top (stop) pair production in a data sample of 1 fb^{-1} collected at a center-of-mass energy of 1.96 TeV with the D0 detector during Run II of the Fermilab Tevatron $p\bar{p}$ collider. The phenomenological framework is the minimal supersymmetric standard model (MSSM) with R-parity conservation. We assume that $BR(\tilde{t}_1 \rightarrow b\ell\tilde{\nu}) = 1$, where $\tilde{\nu}$ is the scalar neutrino (sneutrino). Among possible stop decays [2], this final state is one of the most attractive; in addition to a b quark, it benefits from the presence of a high transverse momentum (p_T) lepton. The sneutrino is either the lightest supersymmetric particle (LSP) or decays invisibly: $\tilde{\nu} \rightarrow \nu\tilde{\chi}_1^0$ or $\nu\tilde{G}$ where the lightest neutralino, $\tilde{\chi}_1^0$, or the gravitino, $\tilde{G}$, is the LSP. We suppose an equal sharing among lepton flavors and consider $\tilde{t}_1\bar{\tilde{t}}_1 \rightarrow b\bar{b}\ell\ell^{'}\tilde{\nu}\tilde{\nu}$ final states, with $\ell\ell^{'} = e^{\pm}\mu^{\mp}$ ($e\mu$ channel) and $\ell\ell^{'} = e^+e^-$ (ee channel). The signal topology consists of two isolated leptons, missing transverse energy ($\not\!\!E_T$), coming mainly from undetected sneutrinos, and jets. A search for stop pair production in the $e\mu$ and $\mu\mu$ ($\tilde{t}_1\bar{\tilde{t}}_1 \rightarrow b\bar{b}\mu\mu\tilde{\nu}\tilde{\nu}$) channels has previously been performed by the D0 collaboration [3] using 428 pb^{-1} of data. The $e\mu$ sample in [3] is a subset of the data sample used in this analysis. Searches for stop pair production in the $b\bar{b}\ell\ell^{'}\tilde{\nu}\tilde{\nu}$ final state have been reported by the ALEPH, L3, and OPAL collaborations [4].

The D0 detector [5] comprises a central tracking system surrounded by a liquid-argon/uranium sampling calorimeter and muon detectors. Charged particles are reconstructed using multi-layer silicon detectors and eight double layers of scintillating fibers in a 2 T magnetic field produced by a superconducting solenoid. After passing through the calorimeter, muons are detected in the muon system comprising three layers of tracking detectors and scintillation counters. Events containing electrons or muons are selected for offline analysis by an online trigger system. A combination of single electron (ee channel) and dilepton ($e\mu$ channel) triggers is used to tag the presence of electrons and muons based on their energy deposition in the calorimeter, hits in the muon detectors, and tracks in the tracking system.

In $p\bar{p}$ collisions, stops are pair-produced via quark-antiquark annihilation and gluon fusion. The $\tilde{t}_1$ pair production cross section, $\sigma_{\tilde{t}_1\bar{\tilde{t}}_1}$, depends primarily on $m_{\tilde{t}_1}$, with only a weak dependence on other MSSM parameters. At $\sqrt{s} = 1.96$ TeV, $\sigma_{\tilde{t}_1\bar{\tilde{t}}_1}$ at next-to-leading-order (NLO), calculated with PROSPINO [6], ranges from 15 pb to 0.5 pb for $100 \leq m_{\tilde{t}_1} \leq 180$ GeV. These cross sections are estimated using CTEQ6.1M parton distribution functions (PDF) [7, 8] and equal renormalization and factorization scales $\mu_{r,f} = m_{\tilde{t}_1}$. A theoretical uncertainty of about 18% is estimated due to scale and PDF choice.

Three-body decays of the stop are simulated using COMPHEP [9] and PYTHIA [10] for parton-level generation and hadronization, respectively. We consider a range of stop mass values from 100 to 200 GeV in steps of 10 GeV. The range of sneutrino masses explored extends from 40 to 140 GeV in steps of 10 to 20 GeV. For each choice of $[m_{\tilde{t}_1}, m_{\tilde{\nu}}]$, 10,000 events are generated. Background processes are simulated using the PYTHIA and ALPGEN [11] Monte Carlo (MC) generators. ALPGEN is interfaced with PYTHIA for parton showering and hadronization. The MC samples use the CTEQ6L PDF and are normalized using next-to-leading order cross sections [12, 13, 14]. All generated events are passed through the full simulation of the detector geometry and response based on GEANT [15]. MC events are then reconstructed and analyzed with the same software as used for the data.

The signal topology depends both on $m_{\tilde{t}_1}$ and on the mass difference $\Delta m = m_{\tilde{t}_1} - m_{\tilde{\nu}}$. The p_T of the leptons and b quarks decrease with smaller values of Δm and $\not\!\!E_T$ values are correlated with $m_{\tilde{t}_1}$ and Δm. For both $e\mu$ and ee channels, the two signal points $[m_{\tilde{t}_1}, m_{\tilde{\nu}}] =$ (140,110) GeV and (170,90) GeV, referred to respectively "Signal A" and "Signal B" in the following, are chosen to illustrate the effect of the selections for low $m_{\tilde{t}_1}$ and low Δm (Signal A) and for high $m_{\tilde{t}_1}$ and high Δm (Signal B).

The main SM background processes mimicking the signal signature are $Z/\gamma^* \rightarrow \tau^+\tau^-$, WW, WZ, ZZ, and $t\bar{t}$ ($e\mu$ and ee decay channels), $Z/\gamma^* \rightarrow e^+e^-$ (ee channel), and instrumental background ($e\mu$ and ee channels). All but the latter are estimated using MC simulations.

Electrons are identified as clusters of energy in calorimeter cells in a cone of size $\mathcal{R} \equiv \sqrt{(\Delta\phi)^2 + (\Delta\eta)^2} = 0.4$ where ϕ is the azimuthal angle and η the pseudorapidity [16]. Electron candidates are required to have a large fraction of their energy deposited in the electromagnetic layers of the calorimeter. The clusters are required to be isolated from hadronic energy depositions, to have a spatially-matched track in the central tracking system with p_T larger than 8 GeV, and to have a shower shape consistent with that of an electron. Electrons are also required to satisfy identification criteria combined in a likelihood variable and based on multivariate discriminators derived from calorimeter shower shape and track variables. Only central electrons ($|\eta| < 1.1$) with transverse energy (E_T) measured in the calorimeter larger than 15 GeV are considered.

Muons are reconstructed by finding tracks pointing to hit patterns in the muon system. Non-isolated muons are

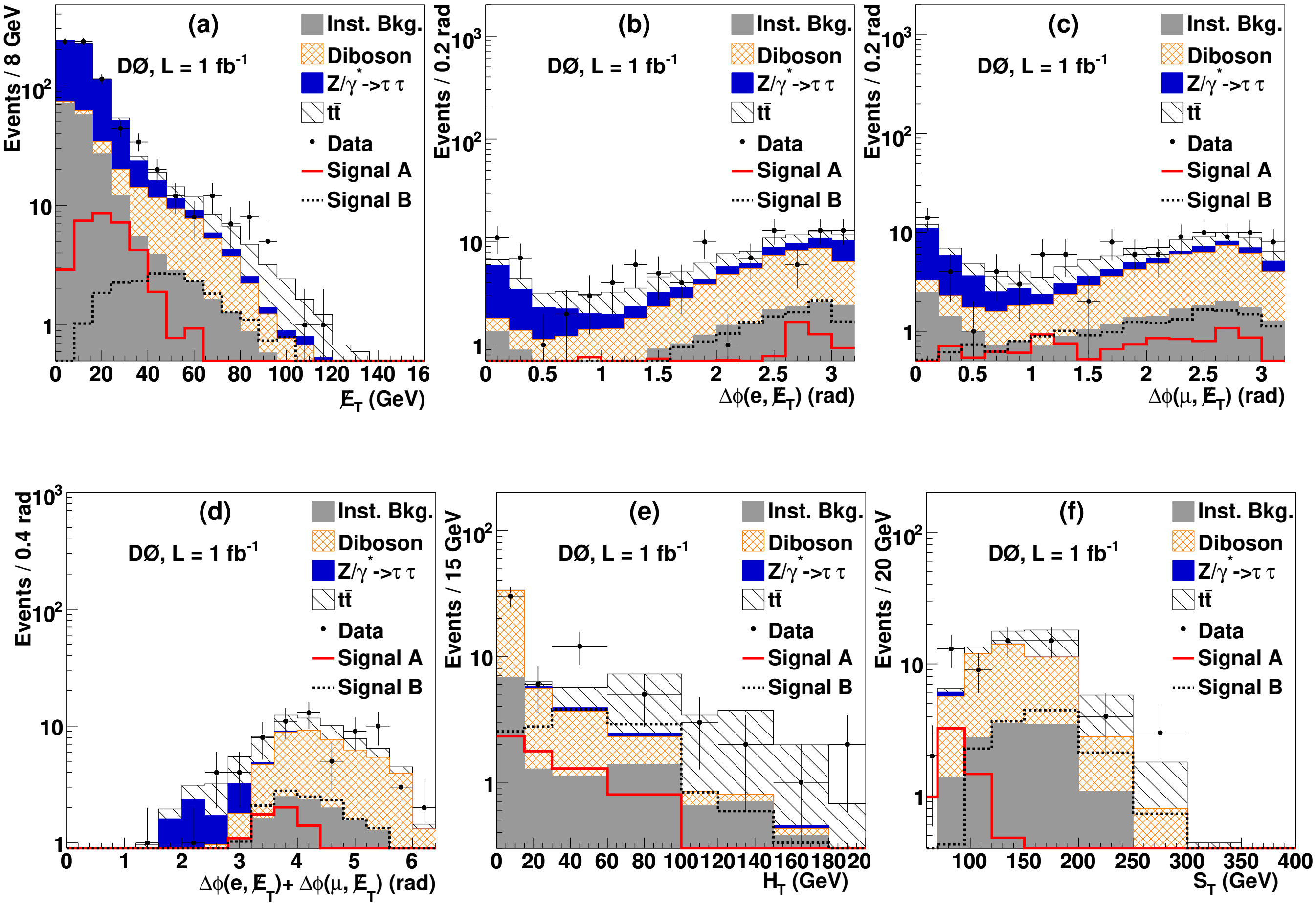

FIG. 1: $e\mu$ channel. Distributions of (a) $\not\!\!E_T$ after preselection, (b) $\Delta\phi(e,\not\!\!E_T)$ and (c) $\Delta\phi(\mu,\not\!\!E_T)$ after Emu 1, (d) $\Delta\phi(e,\not\!\!E_T)$+$\Delta\phi(\mu,\not\!\!E_T)$ after Emu 2, (e) H_T and (f) S_T after Emu 3, for data (dots), expected background (filled areas), and signal expectations for Signal A (solid line) and Signal B (dashed line).

rejected by requiring the sum of the transverse momenta of tracks inside a cone of radius $\mathcal{R} = 0.5$ around the muon direction to be less than 4 GeV, and the sum of transverse energy in the calorimeter in a hollow cone of size $0.1 < \mathcal{R} < 0.4$ around the muon to be less than 4 GeV. To reject cosmic ray muons, requirements on the time of arrival of the muon at the various scintillator layers in the muon system are made. Muons with $|\eta| < 2$ and $p_T > 8$ GeV are considered.

Jets are reconstructed from the energy deposition in the calorimeter towers using the Run II cone algorithm [17] with a radius $\mathcal{R}_{\rm cone} \equiv \sqrt{(\Delta\phi)^2 + (\Delta y)^2} = 0.5$, where y is the rapidity [16]. Jet energies are calibrated to the particle level using correction factors primarily derived from the transverse momentum balance in photon plus jets events. Only jets with $p_T > 15$ GeV and $|\eta| < 2.5$ are considered. The $\not\!\!E_T$ is calculated using all calorimeter cells and is corrected for the jet and electromagnetic energy scales and for the momentum of selected muons.

In each event, the best primary vertex is selected from all reconstructed primary vertices as the one with the smallest probability of originating from a minimum bias interaction [18]. Its longitudinal position with respect to the detector center, z, is restricted to $|z| < 60$ cm to ensure efficient reconstruction. The leptons in an event are required to be isolated from each other ($\mathcal{R}(\ell,\ell') > 0.5$) and from a jet ($\mathcal{R}(\ell,\text{jet}) > 0.5$).

The instrumental background is due to either misidentified electrons or muons, mismeasured $\not\!\!E_T$, or electrons or muons from multijet processes that pass the lepton isolation requirements presented above. Data samples dominated by instrumental background are selected by inverting the muon isolation requirements or the electron-likelihood cut ($e\mu$ channel) or both electron-likelihood criteria (ee channel). The normalization factors for those samples are estimated from data. In the $e\mu$ channel, an exponential fit is performed to the $\not\!\!E_T$ distribution in the range $\not\!\!E_T < 35$ GeV, after subtraction of the MC es-

TABLE I: $e\mu$ channel. Numbers of selected events in data and expected from SM background processes and the two signal samples A and B at the various stages of the analysis. The quoted uncertainties are statistical only.

Selection	Data	Total SM Background	$Z/\gamma^* \to \tau^+\tau^-$	$t\bar{t}$	Diboson	Instrumental	Signal A	Signal B
			Background contributions					
Preselection	735	736 ± 15	458	29.7	60.6	188	34.0 ± 1	26.3 ± 0.7
Emu 1	106	106 ± 5	23	23.5	38.7	21	10.6 ± 0.7	19.4 ± 0.6
Emu 2	71	77 ± 4	5.9	20.0	36.2	15	8.4 ± 0.7	17.6 ± 0.6
Emu 3	61	65 ± 4	0.7	16.4	34.5	13	6.0 ± 0.6	16.1 ± 0.5

timates of the non-instrumental backgrounds, in events containing one electron and one muon. In the ee channel, the normalization is performed using both electron E_T shapes in events containing two electrons in a domain where the instrumental background has a large contribution.

The integrated luminosity [19] of the $e\mu$ data sample is 1100 $\pm$ 67 pb^{-1}. Events are preselected with the requirement that they contain one electron and one muon. To remove a large part of the instrumental background as well as events coming from $Z/\gamma^* \to \tau^+\tau^-$, selections on the $\not\!\!E_T$ [Fig. 1(a)] and on the $\not\!\!E_T$ significance, Signif($\not\!\!E_T$), defined as the ratio of the $\not\!\!E_T$ in an event to its estimated uncertainty given the expected resolutions on the p_T measurements for the selected leptons and jets, are applied:

$$\begin{aligned} \not\!\!E_T &> 30 \text{ GeV} \\ \text{Signif}(\not\!\!E_T) &> 4. \end{aligned} \qquad \text{(Emu 1)}$$

At this stage, the instrumental and $Z/\gamma^* \to \tau^+\tau^-$ events comprise a large part (41%) of the total background. In these processes, reconstructed leptons are correlated with the $\not\!\!E_T$, giving rise to higher event populations at high and low values of the azimuthal angle difference between the leptons and $\not\!\!E_T$, with a low value of the angular difference for one lepton being correlated with a high value for the other. As there is a higher background contribution at low values of the angular distributions [Figs. 1(b) and 1(c)], we require:

$$\begin{aligned} \Delta\phi(\mu, \not\!\!E_T) &> 0.4 \text{ rad} \\ \Delta\phi(e, \not\!\!E_T) &> 0.4 \text{ rad.} \end{aligned} \qquad \text{(Emu 2)}$$

To reduce the $Z/\gamma^* \to \tau^+\tau^-$ background, selections on the transverse mass of the muon and $\not\!\!E_T$ [20], $M_T(\mu, \not\!\!E_T)$, and of the electron and $\not\!\!E_T$, $M_T(e, \not\!\!E_T)$, are applied. To further reduce this background, we use the azimuthal angular differences between the leptons and the missing energy, $\Delta\phi(\mu, \not\!\!E_T)$ and $\Delta\phi(e, \not\!\!E_T)$, which should be large [Fig. 1(d)]. We require:

$$\begin{aligned} M_T(\mu, \not\!\!E_T) &> 20 \text{ GeV} \\ M_T(e, \not\!\!E_T) &> 20 \text{ GeV} \\ \Delta\phi(\mu, \not\!\!E_T) + \Delta\phi(e, \not\!\!E_T) &> 2.9 \text{ rad.} \end{aligned} \qquad \text{(Emu 3)}$$

The number of events surviving at each analysis step for the data, for each background component, and for the two signal samples A and B are summarized in Table I. After all selections, the WW, $t\bar{t}$, and instrumental background contributions dominate. To separate the signal from these backgrounds, two topological variables are used: S_T, defined as the scalar sum of the muon p_T, the electron p_T, and the $\not\!\!E_T$; and H_T, defined as the scalar sum of the transverse momenta of all the jets. WW and instrumental backgrounds populate low values of H_T and S_T while top quark pairs have large values for both variables. The signal distribution depends on the stop mass and on the mass difference Δm, with low values of Δm having low values of H_T and S_T [Figs. 1(e) and 1(f)]. Rather than selecting events using these two variables, the numbers of events predicted for signal and background are compared to the observed numbers in twelve [S_T,H_T] bins (Table II) when extracting limits on the cross section for the $e\mu$ channel.

TABLE II: $e\mu$ channel. Numbers of selected events in data and expected from SM background processes for the twelve S_T and H_T bins. The quoted uncertainties are statistical only.

H_T (GeV)	S_T (GeV) 0–70 Data	0–70 SM	70–120 Data	70–120 SM	>120 Data	>120 SM
0–15	1	0.3 ± 0.3	15	13 ± 2	12	19 ± 2
15–60	1	0.09 ± 0.1	6	4.2 ± 0.9	11	8 ± 1
60–120	0	0.06 ± 0.1	1	1.6 ± 0.6	8	9 ± 1
>120	0	0.01 ± 0.05	0	0.9 ± 0.4	6	7 ± 1

The integrated luminosity of the ee data sample is 1043 $\pm$ 64 pb^{-1}. At preselection, two electrons are required. $Z/\gamma^* \to e^+e^-$ events account for 94% of the total background. While the signal is characterized by the presence of jets originating from the hadronization of b quarks, the $Z/\gamma^* \to e^+e^-$ background owes the presence of jets to gluons from initial state radiation which hadronize into softer jets, resulting in a lower multiplicity of jets. To keep sensivity to low Δm signals while rejecting substantial background, we require at least one

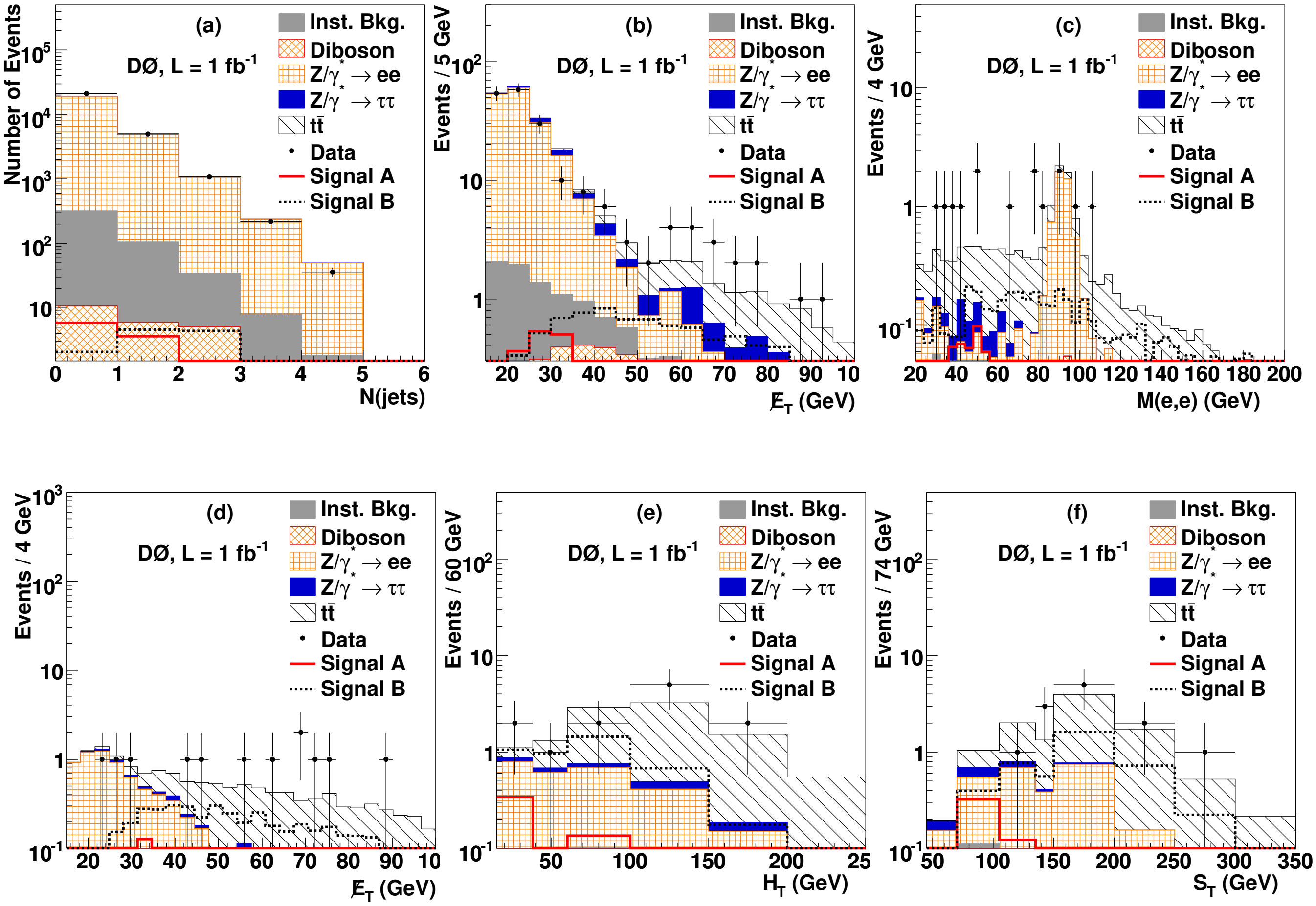

FIG. 2: *ee* channel. Distributions of (a) the number of jets after the preselection, (b) $\not\!\!E_T$ after Dielec 2, (c) the dielectron invariant mass and (d) $\not\!\!E_T$ after Dielec 3, (e) H_T and (f) S_T after Dielec 5, for data (dots), expected background (filled areas), and signal expectations for Signal A (solid line) and Signal B (dashed line).

jet [Fig. 2(a)]:

$$N(\text{jets}) \ \geq \ 1. \qquad \text{(Dielec 1)}$$

To reject contributions from both the instrumental and $Z/\gamma^* \to e^+e^-$ backgrounds, cuts on the $\not\!\!E_T$ and on its significance are performed:

$$\begin{aligned} \not\!\!E_T \ &> \ 15 \text{ GeV} \\ \text{Signif}(\not\!\!E_T) \ &> \ 5. \end{aligned} \qquad \text{(Dielec 2)}$$

At this stage of the analysis,the $Z/\gamma^* \to e^+e^-$ sample is still dominant [Fig. 2(b)] and give rise to higher event populations at high values of the azimuthal angle difference between the two electrons. To remove these events, the following selection is applied:

$$\Delta\phi(ee) \ < \ 3 \text{ rad}. \qquad \text{(Dielec 3)}$$

To increase the search sensitivity in this channel, we take advantage of the presence of jets originating from the fragmentation of long-lived b quarks in the signal. A neural network (NN) tagging tool [21] for heavy flavor that combines information from several lifetime-based b-taggers to maximize the b quark tagging efficiency is used for this purpose. At least one jet in the event is required to be b-tagged (Dielec 4) by satisfying a given NN selection. The b quark tagging operating point preserves high efficiency for the detection of b jets ($\approx 66\%$) with a $\approx 3\%$ probability for a light parton jet to be mistakenly tagged. This point maximizes the sensitivity of the analysis for stop masses of 130 to 140 GeV and for low Δm. At this stage, most of the surviving $Z/\gamma^* \to e^+e^-$ events have a dielectron mass in the vicinity of the Z boson resonance and low $\not\!\!E_T$ values [Figs. 2(c) and 2(d)]. To further suppress this background while preserving the signal, a cut in the plane $[M(e,e),\not\!\!E_T]$ is applied. This selection is optimized for low Δm signals and is defined by:

$$M(e,e) \notin [75, 105] \text{ GeV if } \not\!\!E_T \ < \ 30 \text{ GeV}. \qquad \text{(Dielec 5)}$$

TABLE III: ee channel. Numbers of selected events in data and expected from SM background processes and the two signal samples A and B at the various stages of the analysis. The quoted uncertainties are statistical only.

Selection	Data	Total SM Background	$Z/\gamma^* \to e^+e^-$	$Z/\gamma^* \to \tau^+\tau^-$	$t\bar{t}$	Diboson	Instrumental	Signal A	Signal B
Preselection	27757	25419 ± 87	24810	120	14.1	23.4	452	10.7 ± 0.5	12.7 ± 0.3
Dielec 1	6278	6335 ± 38	6143	29	14.2	12.6	136	4.8 ± 0.4	10.6 ± 0.3
Dielec 2	192	200 ± 5	166	11	12.1	3.9	12	3.0 ± 0.3	8.9 ± 0.2
Dielec 3	142	152 ± 4	122	9.3	11.4	3.5	5.8	2.6 ± 0.3	8.0 ± 0.2
Dielec 4	15	16.0 ± 0.6	6.7	0.5	8.4	0.22	0.17	0.6 ± 0.1	4.7 ± 0.2
Dielec 5	12	12.2 ± 0.4	3.0	0.5	8.4	0.12	0.16	0.6 ± 0.1	4.6 ± 0.2

The selections applied in the ee channel are summarized in Table III along with the number of events surviving at each step for the data, for each background component, and for the two signal samples A and B. A slight excess of data is observed at the preselection level and is due to $Z/\gamma^* \to e^+e^-$ events having no jets and for which the boson transverse momentum is lower than 20 GeV. For these events, the parton showering implemented in the MC generators used in this analysis gives inaccurate results. The $t\bar{t}$ background dominates in the final stage of the selection. Four bins in H_T and S_T [Figs. 2(e) and 2(f) and Table IV] are considered to separate the signal from the SM background.

TABLE IV: ee channel. Numbers of selected events in data and expected from SM background processes for the four S_T and H_T bins. The quoted uncertainties are statistical only.

H_T (GeV)	S_T (GeV) 45–150 Data	45–150 SM	>150 Data	>150 SM
15–60	1	1.9 ± 0.3	2	1 ± 0.1
>60	3	3.3 ± 0.2	6	6 ± 0.2

For both $e\mu$ and ee channels, signal efficiencies, defined with respect to the numbers of events in the relevant channels, reach a value of 10% for large mass differences but decrease to values lower than 0.1% for $\Delta m < 20$ GeV.

The expected numbers of background and signal events depend on several measurements and parametrizations which each introduce a systematic uncertainty: lepton identification and reconstruction efficiency [(1–11)%], trigger efficiency (2%), luminosity (6.1%) [19], instrumental background modeling [(5–18)%], jet energy calibration [(1–11)%], jet identification efficiency and energy resolution [(1–17)%], HF tagging [(2–5)%], and PDF [(5–15)%] uncertainties. These systematic uncertainties (except those for the luminosity and the instrumental background) are obtained by varying sequentially, before any selection, each concerned quantity within one standard deviation. For each channel, the systematic uncertainty on the instrumental background is estimated by varying the fit parameters within one standard deviation of their errors. Higher systematics uncertainties are observed for signal samples with low $m_{\tilde{t}_1}$ and low Δm which give rise to higher event populations at low values of the p_T of the leptons and b quarks.

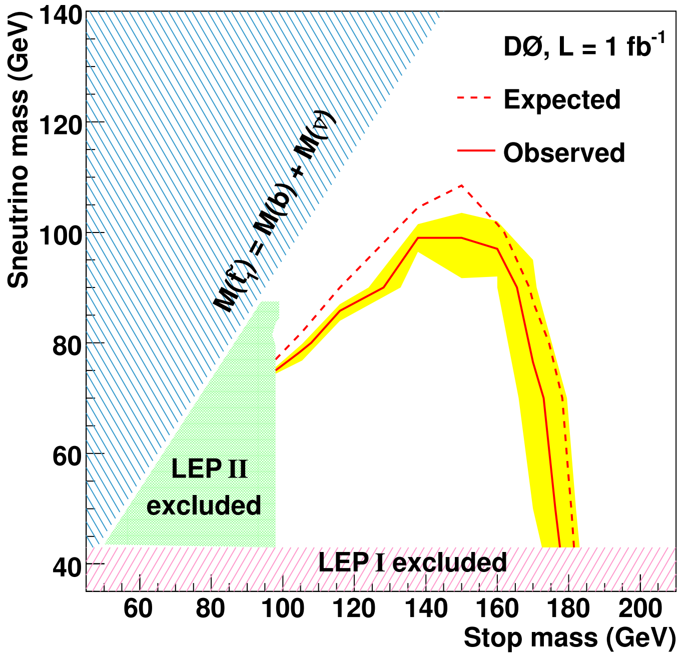

FIG. 3: The 95% C.L. exclusion contour in the sneutrino mass versus stop mass plane. Shaded areas represent the kinematically forbidden region and the LEP I [23] and LEP II [4] exclusions. The dashed and continuous lines represent, respectively, the expected and observed 95% C.L. exclusion limit for this analysis. The band surrounding the observed limit denotes the effect of the uncertainty on the stop production cross section.

No evidence for $\tilde{t}_1$ production is observed after applying all selections for the $e\mu$ and ee data sets. We combine the numbers of expected signal and background events and their corresponding uncertainties, and the number of observed events in data from the twelve bins of the $e\mu$ channel (Table II) and the four bins of the ee channel (Table IV) to calculate upper limits on the signal production cross section at the 95% C.L. for various signal points using the modified frequentist approach [22]. This method employs a likelihood-ratio (LLR) test-statistic, computed under the background-only ($\mathrm{LLR_b}$) or signal plus background ($\mathrm{LLR_{s+b}}$) hypotheses. Simulated pseudo-experiments assuming Poisson statistics and including the effect of systematic uncertainties are generated and distributions for $\mathrm{LLR_b}$ and $\mathrm{LLR_{s+b}}$ are obtained. By integrating the corresponding LLR distributions up to the LLR value observed in data, confidence levels $\mathrm{CL_b}$ and $\mathrm{CL_{s+b}}$ are derived. The stop cross section is varied until the ratio $\mathrm{CL}_s = \mathrm{CL_{s+b}}/\mathrm{CL_b}$ equals 0.05, which defines the 95% C.L. upper limit for the cross section for a given $[m_{\tilde{t}_1}, m_{\tilde{\nu}}]$ point. The intersection of the obtained cross section limit with the theoretical prediction for the cross section as a function of $m_{\tilde{t}_1}$ and $m_{\tilde{\nu}}$ yields the corresponding exclusion point in the $[m_{\tilde{t}_1}, m_{\tilde{\nu}}]$ plane. Correlated uncertainties are taken into account in this calculation; no overlap is expected or observed between the two samples. Figure 3 shows the excluded region as a function of the scalar top quark and sneutrino masses, for nominal (continuous line) and for both minimal and maximal (band surrounding the line) values of $\sigma_{\tilde{t}_1\bar{\tilde{t}}_1}$, corresponding to the estimated theoretical uncertainty. The latter is computed by adding in quadrature the variations corresponding to the PDF uncertainty and the change in renormalization and factorization scale by a factor of two around the nominal value. For larger mass differences between the stop and the sneutrino, a stop mass lower than 175 GeV is excluded. A sensitivity up to $\Delta m = 60$ GeV is observed for stop masses of 150 GeV. Combining the search in the ee final state with the $e\mu$ channel extends the final sensitivity by approximately 5 GeV for large mass differences. The observed limit is within one standard deviation of the expected limit for $m_{\tilde{t}_1} \geq 150$ GeV and within two standard deviations for $m_{\tilde{t}_1} \leq 150$ GeV.

In summary, we presented the results of a search for the pair production of the lightest scalar top quark which decays into $b\ell\tilde{\nu}$. Events with an electron and a muon or with two electrons have been considered in this analysis. No evidence for the lightest stop is observed in this decay, leading to a 95% C.L. exclusion in the $[m_{\tilde{t}_1}, m_{\tilde{\nu}}]$ plane. The largest stop mass excluded is 175 GeV for a sneutrino mass of 45 GeV, and the largest sneutrino mass excluded is 96 GeV for a stop mass of 140 GeV.

We thank the staffs at Fermilab and collaborating institutions, and acknowledge support from the DOE and NSF (USA); CEA and CNRS/IN2P3 (France); FASI, Rosatom and RFBR (Russia); CNPq, FAPERJ, FAPESP and FUNDUNESP (Brazil); DAE and DST (India); Colciencias (Colombia); CONACyT (Mexico); KRF and KOSEF (Korea); CONICET and UBACyT (Argentina); FOM (The Netherlands); STFC (United Kingdom); MSMT and GACR (Czech Republic); CRC Program, CFI, NSERC and WestGrid Project (Canada); BMBF and DFG (Germany); SFI (Ireland); The Swedish Research Council (Sweden); CAS and CNSF (China); and the Alexander von Humboldt Foundation (Germany).

[a] Visitor from Augustana College, Sioux Falls, SD, USA.
[b] Visitor from The University of Liverpool, Liverpool, UK.
[c] Visitor from Rutgers University, Piscataway, NJ, USA.
[d] Visitor from II. Physikalisches Institut, Georg-August-University, Göttingen, Germany.
[e] Visitor from Centro de Investigacion en Computacion - IPN, Mexico City, Mexico.
[f] Visitor from ECFM, Universidad Autonoma de Sinaloa, Culiacán, Mexico.
[g] Visitor from Helsinki Institute of Physics, Helsinki, Finland.
[h] Visitor from Universität Bern, Bern, Switzerland.
[i] Visitor from Universität Zürich, Zürich, Switzerland.
[‡] Deceased.

[1] See, for instance, P. Fayet and S. Ferrara, Phys. Rep. **32**, 249 (1977); H.P. Nilles, Phys. Rep. **110**, 1 (1984).
[2] See, for instance, A. Djouadi and Y. Mambrini, Phys. Rev. Lett. **63**, 115005 (2001) and references therein.
[3] V.M. Abazov *et al.* (D0 Collaboration), Phys. Lett. B **659**, 500 (2008).
[4] LEPSUSYWG Collaboration, ALEPH Collaboration, DELPHI Collaboration, L3 Collaboration, OPAL Collaboration, Note LEPSUSYWG/04-02.1, http://lepsusy.web.cern.ch/lepsusy/www/squarks_summer04/stop_co
[5] V.M. Abazov *et al.* (D0 Collaboration), Nucl. Instrum. Methods Phys. Res. A **565**, 463 (2006).
[6] W. Beenakker *et al.*, Nucl. Phys. **B515**, 453 (1998).
[7] J. Pumplin *et al.*, JHEP **0207**, 012 (2002).
[8] D. Stump *et al.*, JHEP **0310**, 046 (2003).
[9] A. Pukhov *et al.*, User's manual for version 3.3, INP-MSU 98-41/542.
[10] T. Sjöstrand *et al.*, JHEP **05**, 026 (2006); PYTHIA version v6.319 is used.
[11] M.L. Mangano *et al.*, JHEP **0307**, 001 (2003); ALPGEN versions v2.05 and v2.11 are used.
[12] R. Hamberg, W.L. van Neerven, and T. Matsuura, Nucl. Phys. **B359**, 343 (1991) [Erratum-ibid. **B364**, 403 (2002)].
[13] J.M. Campbell and R.K. Ellis, Phys. Rev. D **60**, 113006 (1999).
[14] N. Kidonakis and R. Vogt, Phys. Rev. D **68**, 114014 (2003).
[15] R. Brun and F. Carminati, CERN Program Library Long Writeup W5013, 1993 (unpublished).
[16] The pseudorapidity η is defined as $\eta = -\ln[\tan(\theta/2)]$, with θ being the polar angle with respect to the proton beam direction. The rapidity y is defined as $y = \frac{1}{2}\ln[(E+pz)/(E-pz)]$.
[17] G.C. Blazey *et al.*, arXiv:hep-ex/0005012 (2000).
[18] V.M. Abazov *et al.* (D0 Collaboration), Phys. Rev. D **74**, 112004 (2006).
[19] T. Andeen *et al.*, FERMILAB-TM-2365 (2007).
[20] J. Smith, W.L. van Neerven, and J.A.M. Vermaseren, Phys. Rev. Lett. **50**, 1738 (1983).

[21] T. Scanlon Ph.D. thesis, Imperial College London, FERMILAB-THESIS-2006-43 (2006).
[22] T. Junk, Nucl. Instrum. Methods Phys. Res. A **434**, 435 (1999); A. Read, in "1st Workshop on Confidence Limits," CERN Report No. CERN-2000-005 (2000).
[23] C. Amsler *et al.*, Phys. Lett. B **667**, 1 (2008).